

O(¹D) Kinetic Study of Key Ozone Depleting Substances and Greenhouse Gases

Munkhbayar Baasandorj,^{†,‡,§} Eric L. Fleming,^{§,||} Charles H. Jackman,[§] and James B. Burkholder^{*,†}

[†]Earth System Research Laboratory, Chemical Sciences Division, National Oceanic and Atmospheric Administration, Boulder, Colorado 80305, United States

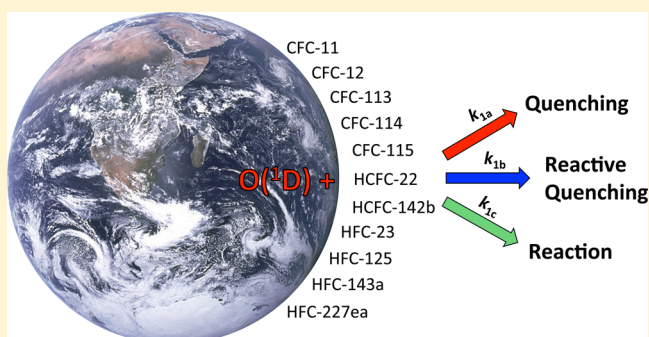
[‡]Cooperative Institute for Research in Environmental Sciences, University of Colorado, Boulder, Colorado 80309, United States

[§]NASA Goddard Space Flight Center, Greenbelt, Maryland 20771, United States

^{||}Science Systems and Applications, Inc., Lanham, Maryland 20706, United States

S Supporting Information

ABSTRACT: A key stratospheric loss process for ozone depleting substances (ODSs) and greenhouse gases (GHGs) is reaction with the O(¹D) atom. In this study, rate coefficients, k , for the O(¹D) atom reaction were measured for the following key halocarbons: chlorofluorocarbons (CFCs) CFCl₃ (CFC-11), CF₂Cl₂ (CFC-12), CFCl₂CF₂Cl (CFC-113), CF₂ClCF₂Cl (CFC-114), CF₃CF₂Cl (CFC-115); hydrochlorofluorocarbons (HCFCs) CHF₂Cl (HCFC-22), CH₃CClF₂ (HCFC-142b); and hydrofluorocarbons (HFCs) CHF₃ (HFC-23), CHF₂CF₃ (HFC-125), CH₃CF₃ (HFC-143a), and CF₃CHFCF₃ (HFC-227ea). Total rate coefficients, k_T , corresponding to the loss of the O(¹D) atom, were measured over the temperature range 217–373 K using a competitive reactive technique. k_T values for the CFC and HCFC reactions were $>1 \times 10^{-10} \text{ cm}^3 \text{ molecule}^{-1} \text{ s}^{-1}$, except for CFC-115, and the rate coefficients for the HFCs were in the range $(0.095\text{--}0.72) \times 10^{-10} \text{ cm}^3 \text{ molecule}^{-1} \text{ s}^{-1}$. Rate coefficients for the CFC-12, CFC-114, CFC-115, HFC-23, HFC-125, HFC-143a, and HFC-227ea reactions were observed to have a weak negative temperature dependence, $E/R \approx -25 \text{ K}$. Reactive rate coefficients, k_R , corresponding to the loss of the halocarbon, were measured for CFC-11, CFC-115, HCFC-22, HCFC-142b, HFC-23, HFC-125, HFC-143a, and HFC-227ea using a relative rate technique. The reactive branching ratio obtained was dependent on the composition of the halocarbon and the trend in O(¹D) reactivity with the extent of hydrogen and chlorine substitution is discussed. The present results are critically compared with previously reported kinetic data and the discrepancies are discussed. 2D atmospheric model calculations were used to evaluate the local and global annually averaged atmospheric lifetimes of the halocarbons and the contribution of O(¹D) chemistry to their atmospheric loss. The O(¹D) reaction was found to be a major global loss process for CFC-114 and CFC-115 and a secondary global loss process for the other molecules included in this study.



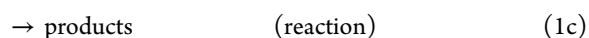
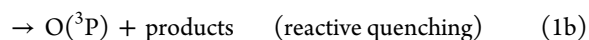
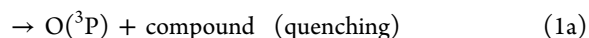
1. INTRODUCTION

Accurate climate change modeling relies on accurate input kinetic and photochemical parameters for the atmospheric loss processes of key ozone depleting substances (ODSs) and greenhouse gases (GHGs). Quantifying the atmospheric loss processes of ODSs and GHGs is essential for determining their atmospheric lifetimes and, thus, evaluating their long-term impact on the environment and climate system. A key stratospheric loss process for trace species is gas-phase reaction with the O(¹D) atom. As a result, O(¹D) kinetics of atmospherically relevant compounds have been studied over the years using a variety of experimental techniques (see the NASA/JPL Chemical Kinetics and Photochemical Data Evaluation¹ for an overview of O(¹D) atmospherically relevant kinetic studies). In spite of these efforts, the kinetic parameters for several key halocarbon compounds still have a relatively

high degree of uncertainty, which impacts the accuracy with which their atmospheric lifetimes, ozone depletion potentials (ODPs), and global warming potentials (GWPs) can be calculated.

O(¹D) atom reactions proceed via several product channels

O(¹D) + compound



Received: December 27, 2012

Revised: February 23, 2013

Published: February 26, 2013

where in this study “compound” represents a ODS or GHG halocarbon. The branching ratios for the channels in reaction 1 and the products formed are dependent on the chemical composition of the molecule, i.e., the presence of H, F, and Cl atoms in the halocarbon. The total rate coefficient for reaction 1, k_T , which corresponds to the loss of the O(¹D) atom, is defined as $k_T = k_{1a} + k_{1b} + k_{1c}$ and the reactive rate coefficient, k_R , i.e., the loss of the halocarbon, is given by $k_R = k_{1b} + k_{1c}$. The reactive rate coefficient is of particular interest in atmospheric modeling in that it leads to the removal of the halocarbon from the atmosphere and the activation of reactive chlorine for chlorofluorocarbons (CFCs) and hydrochlorofluorocarbons (HCFCs). The uncertainties in the currently available rate coefficient data and a lack of experimental data, in some cases, has led the recommendations for use in atmospheric models¹ to have relatively large uncertainties at the temperatures most relevant to stratospheric chemistry; uncertainty factors of 2–4 are recommended for the low temperature rate coefficients in many cases.

In this study, total rate coefficients for the O(¹D) reaction with CFCl₃ (CFC-11), CF₂Cl₂ (CFC-12), CFCl₂CF₂Cl (CFC-113), CF₂ClCF₂Cl (CFC-114), CF₃CF₂Cl (CFC-115), CHF₂Cl (HCFC-22), CH₃CClF₂ (HCFC-142b), CHF₃ (HFC-23), CHF₂CF₃ (HFC-125), CH₃CF₃ (HFC-143a), and CF₃CHF₂CF₃ (HFC-227ea) were measured at temperatures in the range 217–373 K using a competitive reaction method. The rate coefficient temperature dependence for these reactions was expected to be weak over the temperature range that is most relevant to atmospheric chemistry. However, the lack of experimental data has led to relatively large estimated uncertainties in the O(¹D) rate coefficients and, thus, the need for experimental temperature dependent data.

Reactive rate coefficients, k_R , were measured for the O(¹D) reactions with CFCl₃ (CFC-11), CF₃CF₂Cl (CFC-115), CHF₂Cl (HCFC-22), CH₃CClF₂ (HCFC-142b), CHF₃ (HFC-23), CHF₂CF₃ (HFC-125), CH₃CF₃ (HFC-143a), and CF₃CHF₂CF₃ (HFC-227ea) using a relative rate method at 296 K, except for the CFCl₃ (CFC-11) reaction, which was also measured at 240 K. The results from the laboratory kinetic measurements were used as input to the Goddard Space Flight Center (GSFC) 2D atmospheric model^{2,3} to evaluate the potential impact of the present kinetic results on the local and global annually averaged atmospheric lifetimes for these compounds, the fractional contribution of the O(¹D) reaction to their atmospheric loss, as well as the range of uncertainty in the calculated lifetime due to uncertainties in the O(¹D) kinetic parameters.

2. EXPERIMENTAL DETAILS

Two independent experimental methods were used in this study to measure rate coefficients for the reaction of O(¹D) with a series of halocarbons. In total 11 halocarbons were studied as given earlier and listed in Table 1 including 5 chlorofluorocarbons (CFCs), 2 hydrochlorofluorocarbons (HCFCs), and 4 hydrofluorocarbons (HFCs). Reactive rate coefficients, k_R , were measured using a relative rate method with Fourier transform infrared spectroscopy (FTIR) used to measure the loss of the halocarbon and reference compound. Total rate coefficients, $k_T(T)$, were measured over a range of temperature, 217–373 K, at ~35 Torr (He) total pressure using a competitive reaction method. The experimental methods are described separately below.

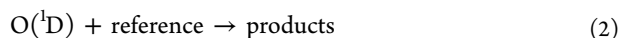
Table 1. Summary of Experimental Conditions and Total Rate Coefficients, $k_T(T)$, i.e., O(¹D) Loss, Obtained in This Work for the O(¹D) + Halocarbon Reactions^a

halocarbon	temp (K)	concn range (10 ¹⁴ molecules cm ⁻³)	$k_T(T)^b$ (10 ⁻¹⁰ cm ³ molecule ⁻¹ s ⁻¹)
CFCl ₃ CFC-11	217	0.21–0.94	2.32 ± 0.20
	241	0.33–1.06	2.39 ± 0.20
	296	0.26–2.14	2.35 ± 0.18
	339	0.25–1.43	2.48 ± 0.21
	372	0.22–1.21	2.41 ± 0.20
CF ₂ Cl ₂ CFC-12	217	0.25–0.94	1.68 ± 0.14
	241	0.28–1.02	1.62 ± 0.16
	296	0.27–1.50	1.57 ± 0.13
	339	0.28–1.23	1.60 ± 0.14
	372	0.24–1.20	1.59 ± 0.13
CFCl ₂ CF ₂ Cl CFC-113	217	0.23–0.89	2.21 ± 0.18
	240	0.21–0.84	2.33 ± 0.20
	296	0.23–1.03	2.43 ± 0.16
	373	0.16–0.94	2.30 ± 0.20
	373	0.16–0.94	2.30 ± 0.20
CF ₂ ClCF ₂ Cl CFC-114	217	0.23–0.93	1.42 ± 0.12
	241	0.28–1.17	1.49 ± 0.12
	296	0.22–1.22	1.43 ± 0.09
	337	0.28–1.10	1.46 ± 0.11
	373	0.16–0.94	1.34 ± 0.11
CF ₃ CF ₂ Cl CFC-115	217	0.23–0.93	0.752 ± 0.069
	241	0.92–2.26	0.743 ± 0.070
	296	0.67–1.22	0.702 ± 0.054
	373	0.16–0.94	0.719 ± 0.060
	373	0.16–0.94	0.719 ± 0.060
CHClF ₂ HCFC-22	217	0.74–1.95	1.115 ± 0.064
	241	0.64–2.58	0.989 ± 0.049
	296	0.22–1.22	0.996 ± 0.074
	373	0.40–1.70	1.088 ± 0.104
	373	0.40–1.70	1.088 ± 0.104
CH ₃ CClF ₂ HCFC-142b	217	0.24–1.07	1.72 ± 0.10
	241	0.30–1.11	1.79 ± 0.10
	296	0.23–1.01	1.86 ± 0.09
	373	0.28–0.85	1.78 ± 0.16
	373	0.28–0.85	1.78 ± 0.16
CHF ₃ HFC-23	217	8.54–22.3	0.100 ± 0.007
	240	5.32–22.8	0.100 ± 0.008
	296	4.73–33.0	0.096 ± 0.007
	352	4.23–30.7	0.095 ± 0.005
	372	4.87–26.8	0.095 ± 0.006
CHF ₂ CF ₃ HFC-125	217	7.02–16.4	0.108 ± 0.008
	241	7.34–25.0	0.104 ± 0.007
	296	7.16–28.6	0.101 ± 0.004
	373	4.69–17.3	0.103 ± 0.007
	373	4.69–17.3	0.103 ± 0.007
CH ₃ CF ₃ HFC-143a	217	0.42–2.47	0.721 ± 0.035
	241	0.62–2.91	0.691 ± 0.053
	296	0.37–3.23	0.708 ± 0.044
	336	0.48–2.60	0.702 ± 0.060
	373	0.58–3.29	0.680 ± 0.040
CF ₃ CHF ₂ CF ₃ HFC-227ea	217	6.27–19.8	0.107 ± 0.006
	241	5.47–29.4	0.110 ± 0.009
	296	7.16–28.6	0.097 ± 0.006
	373	4.69–17.3	0.096 ± 0.008
	373	4.69–17.3	0.096 ± 0.008

^aOther experimental conditions: [*n*-C₄H₁₀] (reference compound) in the range (0.7–2) × 10¹³ molecules cm⁻³; [O₃] in the range (4–8) × 10¹² molecules cm⁻³, and 30 to 40 Torr (He) total pressure.

^bUncertainties are at the 2σ level from the precision of the linear least-squares fit of the data.

2.1. Relative Rate Method. Reactive rate coefficients, k_R , were measured relative to that of a reference compound



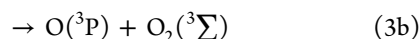
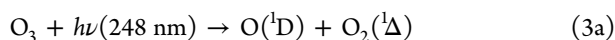
by measuring the simultaneous loss of the reactant and reference compound. Experiments were performed using an apparatus described in greater detail in previous studies from this laboratory.^{4,5} The apparatus consisted of a Pyrex reactor (100 cm long, 5 cm i.d.) coupled to an external FTIR absorption cell at 296 K. The FTIR was used to measure the loss of the reactant and reference compounds.

Provided that the reactant and reference (ref) compounds are lost solely via reaction with $\text{O}(^1\text{D})$ the rate coefficients for the reactant and reference compound are related by

$$\frac{k_{\text{R}}(\text{reactant})}{k_{\text{R}}(\text{ref})} = \frac{\ln([\text{reactant}]_0/[\text{reactant}]_t)}{\ln([\text{ref}]_0/[\text{ref}]_t)} \quad (1)$$

where $[\text{reactant}]_0$ and $[\text{ref}]_0$ are the initial reactant and reference compound concentrations and $[\text{reactant}]_t$ and $[\text{ref}]_t$ are the concentrations at time t . In an attempt to minimize systematic errors in $k_{\text{R}}(\text{reactant})$, experiments were performed using multiple reference compounds in many cases. The reference compounds used in this study were N_2O , NF_3 , CHF_2Cl (HCFC-22), and $\text{CF}_3\text{CF}_2\text{Cl}$ (CFC-115).

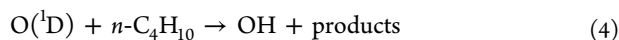
Experiments were performed by first mixing the reactant and reference compounds in the reactor by circulating the gases between the reactor and infrared absorption cell using a Teflon diaphragm pump at a total pressure of ~ 180 Torr (He bath gas). The initial reactant and reference concentrations in the mixture were measured by infrared absorption using a multipass absorption cell with a 360 cm path length. Infrared spectra were recorded at a spectral resolution of 1 cm^{-1} between 500 and 4000 cm^{-1} with 100 coadded scans. Ozone was then added slowly to the reaction mixture by passing a small flow of He through a 195 K silica-gel trap containing O_3 . $\text{O}(^1\text{D})$ radicals were produced in the reactor by passing the output of a pulsed KrF excimer laser (248 nm) along the length of the reactor



where the $\text{O}(^1\text{D})$ yield is 0.9.¹ The photolysis laser fluence was measured at the exit of the reactor and was varied between 10 and $40\text{ mJ cm}^{-2}\text{ pulse}^{-1}$ over the course of the study. The O_3 steady-state concentration in these experiments was $(1\text{--}6) \times 10^{14}\text{ molecules cm}^{-3}$. The halocarbon concentrations were in the range $(3\text{--}8) \times 10^{14}\text{ molecules cm}^{-3}$ and the N_2O concentration was $\sim 2 \times 10^{15}\text{ molecules cm}^{-3}$. The system pressure increased over the course of the experiment from 100 to ~ 600 Torr (He) due to the addition of the O_3/He mixture. The loss of the reactant and reference compounds was measured while circulating the gas mixture.

In the absence of O_3 the reactant and reference compounds were found to be stable with respect to a change in total pressure, exposure to the photolysis laser beam, and gas circulation over the duration of a typical experiment, with $<0.4\%$ change in the reactant concentrations. The reaction mixtures were also stable when O_3 was added to the mixture, but with the photolysis laser off.

2.2. Competitive Reaction Method. In the competitive reaction method, OH radicals were produced by the reaction of $\text{O}(^1\text{D})$ with $n\text{-C}_4\text{H}_{10}$ (n -butane)



and monitored using laser induced fluorescence (LIF). That is, $\text{O}(^1\text{D})$ atoms were not detected directly, but $\text{O}(^1\text{D})$ atoms were converted to OH radicals whose temporal profile was measured by LIF. Total rate coefficients were determined from an analysis of the OH radical temporal profiles in the presence of known concentrations of the halocarbon. The experimental apparatus^{5–7} and methods^{5,8} employed have been used in previous studies from this laboratory and are described in greater detail elsewhere. A brief summary is presented here.

OH temporal profiles were measured using laser induced fluorescence (LIF) following excitation of the $\text{A}^2\Sigma^+(\nu=1) \leftarrow \text{X}^2\Pi(\nu=0)$ transition at $\sim 282\text{ nm}$ using the frequency doubled output from a pulsed Nd:YAG pumped dye laser. OH fluorescence was detected using a photomultiplier tube (PMT) after it passed through a band-pass filter (308 nm, fwhm = 10 nm). The delay time between the photolysis and the probe lasers, i.e., the reaction time, was typically varied over the range 10–1000 μs .

$\text{O}(^1\text{D})$ radicals were produced in the 248 nm (KrF excimer laser) pulsed laser photolysis of O_3 , reaction 3. The photolysis laser fluence was monitored at the exit of the reactor and was varied between 10 and $30\text{ mJ cm}^{-2}\text{ pulse}^{-1}$ over the course of the study. The initial $\text{O}(^1\text{D})$ concentration was estimated to be in the range $(1\text{--}5) \times 10^{12}\text{ molecules cm}^{-3}$.

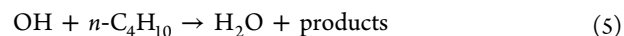
The OH temporal profiles were described by a biexponential expression

$$S_{\text{OH}}(t) = C[\exp(-k'_{\text{Loss}}t) - \exp(-k'_{\text{Rise}}t)] \quad (\text{II})$$

where $S_{\text{OH}}(t)$ is the OH radical fluorescence signal at time t , C is a constant that is proportional to the total OH radical concentration, and k'_{Loss} and k'_{Rise} are the pseudo-first-order rate coefficients for the loss and formation of the OH radical, respectively. The rate of the initial rise in the OH radical concentration is a measure of the pseudo-first-order loss of $\text{O}(^1\text{D})$ in the system

$$\begin{aligned} k'_{\text{Rise}} &= k_4[n\text{-C}_4\text{H}_{10}] + k_{\text{O}(^1\text{D})+\text{O}_3}[\text{O}_3] + k'_b + k_{\text{T}}[\text{reactant}] \\ &= k_0 + k_{\text{T}}[\text{reactant}] \end{aligned} \quad (\text{III})$$

where k'_b is the pseudo-first-order rate coefficient for $\text{O}(^1\text{D})$ loss due to reaction with background impurities and diffusion out of the detection volume. k'_{Loss} was primarily determined by the reaction of the OH radical with n -butane



where $k_5 = 2.35 \times 10^{-12}\text{ cm}^3\text{ molecule}^{-1}\text{ s}^{-1}$ ⁹ and partially due to diffusion out of the detection volume. Under the conditions of our experiments k'_{Loss} was typically $<100\text{ s}^{-1}$.

Total rate coefficients were determined from a nonlinear least-squares analysis of a series of OH temporal profiles measured with different halocarbon concentrations. $[n\text{-C}_4\text{H}_{10}]$, $[\text{O}_3]$, and total pressure were held nearly constant during the measurement of the OH temporal profiles. The reactant concentration was typically varied over the range $(1\text{--}6) \times 10^{14}\text{ molecules cm}^{-3}$. The n -butane and O_3 concentrations were determined from the measured gas flows and pressure to be $(0.7\text{--}2) \times 10^{13}\text{ molecules cm}^{-3}$ and $(4\text{--}8) \times 10^{12}\text{ molecules cm}^{-3}$, respectively, and the reactor pressure was in the range 30–40 Torr (He). The halocarbon concentration was determined from measured flows and pressures as well as online infrared absorption. The two concentration determination methods agreed to better than 5%. A linear least-squares analysis of $(k'_{\text{Rise}} - k_0)$

Table 2. Total Rate Coefficients for the O(¹D) + Halocarbon Reactions Obtained in This Work and Reported in Previous Studies^a

haocarbon	temp range (K)	$k(296\text{ K})^b$ ($10^{-10}\text{ cm}^3\text{ molecule}^{-1}\text{ s}^{-1}$)	A^c ($10^{-10}\text{ cm}^3\text{ molecule}^{-1}\text{ s}^{-1}$)	E/R^c (K)	exptl method/uncertainty ^d	ref
CFCl ₃ CFC-11	173–343	2.2 ± 0.7	2.2	0	E	Davidson et al. ¹⁰
	298	2.4 ± 0.2			RA	Force and Wiesenfeld ¹¹
		2.3 (+1.0/−0.7)	2.3	0	Rec; $f(298\text{ K})^2 = 1.44$, $2g = 100$	NASA/JPL eval ¹
CF ₂ Cl ₂ CFC-12	217–373	2.35 ± 0.18	2.39 ± 0.20	0 ± 25	CR; $f(298\text{ K})^2 = 1.14$, $2g = 0$	this work
	173–343	1.45 ± 0.5	1.45	0	E	Davidson et al. ¹⁰
	298	1.4 ± 0.2			RA	Force and Wiesenfeld ¹¹
CFCl ₂ CF ₂ Cl CFC-113		1.4 (+0.8/−0.5)	1.4	0	Rec; $f(298\text{ K})^2 = 1.56$, $2g = 100$	NASA/JPL eval ¹
	217–373	1.57 ± 0.13	1.47 ± 0.12	−(25 ± 8)	CR; $f(298\text{ K})^2 = 1.12$, $2g = 0$	this work
	298	2 (+2.5/−1.1)	2	0	Rec; $f(298\text{ K})^2 = 2.25$, $2g = 100$	NASA/JPL eval ¹
CF ₂ ClCF ₂ Cl CFC-114		2.33 ± 0.40			CR	Baasandorj et al. ⁸
	217–373	2.43 ± 0.16	2.32 ± 0.20	0 ± 50	CR; $f(298\text{ K})^2 = 1.14$, $2g = 0$	this work
	298	1.32 ± 0.07			RF	Ravishankara et al. ¹⁴
CF ₃ CF ₂ Cl CFC-115		1.42 ± 0.25			CR	Baasandorj et al. ⁸
	298	1.3 (+0.6/−0.4)	1.3	0	Rec; $f(298\text{ K})^2 = 1.44$, $2g = 100$	NASA/JPL eval ¹
	217–373	1.43 ± 0.09	1.30 ± 0.20	−(25 ± 50)	CR; $f(298\text{ K})^2 = 1.14$, $2g = 0$	this work
CHF ₂ Cl HCFC-22	298	0.50 ± 0.04			RF	Ravishankara et al. ¹⁴
		0.5 (+0.22/−0.15)	0.5	0	Rec; $f(298\text{ K})^2 = 1.44$, $2g = 50$	NASA/JPL eval ¹
	217–373	0.702 ± 0.054	0.65 ± 0.07	−(30 ± 30)	CR; $f(298\text{ K})^2 = 1.14$, $2g = 0$	this work
CH ₃ CF ₂ Cl HCFC-142b	173–343	0.95 ± 0.30	0.95	0	E	Davidson et al. ¹⁰
	298	1.08 ± 0.20			RF	Warren et al. ¹⁵
		1.0 (+0.32/−0.24)	1.0	0	Rec; $f(298\text{ K})^2 = 1.32$, $2g = 100$	NASA/JPL eval ¹
CHF ₃ HFC-23	217–373	0.996 ± 0.074	1.04 ± 0.35	0 ± 100	CR; $f(298\text{ K})^2 = 1.17$, $2g = 0$	this work
		2.15 ± 0.20			RF	Warren et al. ¹⁵
		2.2 (+0.97/−0.67)	2.2	0	Rec; $f(298\text{ K})^2 = 1.44$, $2g = 100$	NASA/JPL eval ¹
CHF ₂ CF ₃ HFC-125	217–373	1.86 ± 0.09	1.80 ± 0.12	0 ± 45	CR; $f(298\text{ K})^2 = 1.14$, $2g = 0$	this work
	298	0.084 ± 0.008			RA	Force and Wiesenfeld ¹¹
	298	0.098 ± 0.006			RF	Schmoltner et al. ¹⁸
CH ₃ CF ₃ HFC-143a		0.091 (+0.019/−0.016)	0.091	0	Rec; $f(298\text{ K})^2 = 1.21$, $2g = 100$	NASA/JPL eval ¹
	217–373	0.096 ± 0.007	0.087 ± 0.003	−(30 ± 10)	CR; $f(298\text{ K})^2 = 1.10$, $2g = 0$	this work
	298	1.23 ± 0.06			RF	Warren et al. ¹⁵
CF ₃ CHFCF ₃ HFC-227ea		0.10 (+0.1/−0.05)			LIF	Kono and Matsumi ¹⁹
	217–373	1.2 (+0.39/−0.29)	1.2	0	Rec; $f(298\text{ K})^2 = 1.32$, $2g = 100$	NASA/JPL eval ¹
	298	0.101 ± 0.004	0.095 ± 0.011	−(25 ± 30)	CR; $f(298\text{ K})^2 = 1.14$, $2g = 0$	this work
CF ₃ CHFCF ₃ HFC-227ea	298 ^e	0.40 ± 0.05			LIF	Kono and Matsumi ¹⁹
		0.44 (+0.55/−0.24)	0.44	0	Rec; $f(298\text{ K})^2 = 2.25$, $2g = 50$	NASA/JPL Eval. ¹
	217–373	0.708 ± 0.044	0.65 ± 0.06	−(20 ± 25)	CR; $f(298\text{ K})^2 = 1.14$, $2g = 0$	this work
CF ₃ CHFCF ₃ HFC-227ea					Rec	NASA/JPL eval ¹
	217–373	0.0975 ± 0.006	0.079 ± 0.016	−(70 ± 50)	CR; $f(298\text{ K})^2 = 1.2$, $2g = 0$	this work

^aCR: competitive reaction method. LIF: laser induced fluorescence. RF: resonance fluorescence. RA: resonance absorption. E: emission. Rec: recommendation. All experimental studies used pulsed laser photolysis methods to produce O(¹D) atoms. The Davidson et al. reported value is the average of values obtained over the specified temperature range (no temperature dependence was observed within the precision of the measurements). ^bUncertainties in this work at the 2σ level from the precision of the measurement. ^cUncertainties at the 2σ level from the precision of the fit. ^dThe uncertainty parameters $f(298\text{ K})$ and g are defined as $f(T) = f(298\text{ K}) \exp[\lg[(1/T) - (1/298)]]$, where $f(T)$ is an uncertainty factor for $k(T)$, $f(298\text{ K})$ is the 1σ estimated uncertainty factor for the room temperature rate coefficient, $k(298\text{ K})$, and g is a parameter used to describe the increase in uncertainty at temperatures other than 298 K. The 2σ uncertainties are given as $f(298\text{ K})^2$ and $2g$. The $f(298\text{ K})^2$ values for “this work” are estimated from the range in the experimental data obtained at all temperatures (see Supporting Information for Arrhenius plots). ^eReported as “room temperature”.

versus [halocarbon] yielded the bimolecular total rate coefficient for the O(¹D) + halocarbon reaction.

2.3. Materials. He (UHP, 99.999%) was passed through a molecular sieve trap at liquid nitrogen temperature prior to entering the vacuum systems. CFCl₃, CF₂Cl₂, CFCl₂CF₂Cl, CF₂ClCF₂Cl, CF₃CF₂Cl, CHF₂Cl, CH₃CF₂Cl, CHF₃, CHF₂CF₃, CF₃CH₃, and CF₃CHFCF₃ samples (≥99%) were degassed in freeze–pump–thaw cycles during mixture preparation. NF₃ (electronic grade, 99.99%), N₂O (99.99%), and *n*-C₄H₁₀ (n-butane, 99.93%) samples were degassed in freeze–pump–thaw cycles during mixture preparation. Dilute mixtures of the compounds were prepared manometrically in

12 L Pyrex bulbs. Ozone was produced by flowing O₂ through a commercial ozonizer and collected in a silica gel trap at 195 K. Dilute mixtures of O₃ in He (~0.1%) were prepared off-line in a 12 L Pyrex bulb for use in the LIF experiments. FTIR absorption measurements were used to periodically measure the O₃ mixing ratio during the course of the study.

Gas flows were measured with calibrated electronic mass flow meters and pressures were measured using 10, 100, and 1000 Torr capacitance manometers. The photolysis and probe lasers were operated at 10 Hz repetition rate. The gas flow velocity, 9–16 cm s^{−1}, ensured a fresh sample of gas in the LIF reaction volume for each photolysis pulse. The gas circulation in the

Table 3. Reactive Rate Coefficient, k_R Results at 296 K for the $O(^1D)$ + Halocarbon Reactions Included in This Work

halocarbon	compound	reference compound		$k_R(\text{ref})$ source	$k_R/k_R(\text{ref})^b$	k_R^b ($10^{-10} \text{ cm}^3 \text{ molecule}^{-1} \text{ s}^{-1}$)
		compound	$k_R(\text{ref})$ ($10^{-10} \text{ cm}^3 \text{ molecule}^{-1} \text{ s}^{-1}$) ^a			
CFCl ₃	CFC-11	N ₂ O	1.27 ± 0.25	NASA/JPL ¹	1.66 ± 0.07	2.11 ± 0.09
		N ₂ O	1.29 ± 0.25 ^c	NASA/JPL ¹	1.74 ± 0.04	2.24 ± 0.05 ^c
CF ₃ CF ₂ Cl	CFC-115	NF ₃	0.22 ± 0.03	Baasandorj et al. ⁵	2.32 ± 0.06	0.510 ± 0.013
		CF ₃ CHF ₂ (HFC-125)	0.0733 ± 0.009	this work	7.22 ± 0.45	0.529 ± 0.033
		CHClF ₂ (HCFC-22)	0.770 ± 0.013	this work	0.662 ± 0.010	0.510 ± 0.008
						0.516 ± 0.018 (avg)
CHClF ₂	HCFC-22	NF ₃	0.22 ± 0.03	Baasandorj et al. ⁵	3.50 ± 0.06	0.770 ± 0.013
CH ₃ CF ₂ Cl	HCFC-142b	CHClF ₂ (HCFC-22)	0.770 ± 0.013	this work	1.38 ± 0.03	1.06 ± 0.023
		CF ₃ CF ₂ Cl (CFC-115)	0.516 ± 0.018	this work	2.23 ± 0.03	1.15 ± 0.015
						1.11 ± 0.027 (avg)
CHF ₃	HFC-23	NF ₃	0.22 ± 0.03	Baasandorj et al. ⁵	0.105 ± 0.002	0.0235 ± 0.0040
CF ₃ CHF ₂	HFC-125	NF ₃	0.22 ± 0.03	Baasandorj et al. ⁵	0.365 ± 0.030	0.0795 ± 0.0070
		CHF ₃ (HFC-23)	0.0235 ± 0.0040	this work	2.86 ± 0.14	0.0672 ± 0.0066
						0.0733 ± 0.009 (avg)
CH ₃ CF ₃	HFC-143a	NF ₃	0.22 ± 0.03	Baasandorj et al. ⁵	1.93 ± 0.04	0.423 ± 0.008
		CF ₃ CF ₂ Cl (CFC-115)	0.516 ± 0.018	this work	0.74 ± 0.03	0.380 ± 0.015
		CHClF ₂ (HCFC-22)	0.770 ± 0.013	this work	0.49 ± 0.01	0.370 ± 0.015
						0.391 ± 0.011 (avg)
CF ₃ CHFCF ₃	HFC-227ea	NF ₃	0.22 ± 0.03	Baasandorj et al. ⁵	0.31 ± 0.033	0.0677 ± 0.0070
		CHF ₃ (HFC-23)	0.0235 ± 0.0040	this work	3.02 ± 0.22	0.0696 ± 0.0053
		CF ₃ CHF ₂ (HFC-125)	0.0733 ± 0.009	this work	0.99 ± 0.06	0.0725 ± 0.0044
						0.0699 ± 0.005 (avg)

^aUncertainties in reported literature values are 2σ , where NASA/JPL¹ reports an absolute uncertainty and Baasandorj et al.⁵ reports the precision of their relative rate measurement. The 2σ uncertainties from “this work” were taken from the measurement precision reported in the final column.

^bUncertainties are 2σ from the precision of the measurement. ^cReference rate coefficient and measurement at 240 K.

relative rate experiments was $\sim 12 \text{ L min}^{-1}$ with a $\sim 6 \text{ s}$ residence time in the reaction cell. The uncertainties quoted throughout this paper are 2σ (95% confidence level) unless stated otherwise.

3. RESULTS AND DISCUSSION

In this section the kinetic results obtained for the CFC, HCFC, and HFC compounds included in this study are presented and compared with previously reported values, where available. Discrepancies among previously reported total and reactive rate coefficients were resolved in many cases as a result of this work, in particular large discrepancies existing for the CHF₂CF₃ (HFC-125) and CF₃CF₂Cl (CFC-115) reactions were resolved. Rate coefficient data are reported for CF₃CHFCF₃ (HFC-227ea) for which there were no previous measurements available. The kinetic results from this work are summarized in Tables 1–4. The uncertainties in $k_T(T)$ and k_R , based on the precision and accuracy of the present measurements, are significantly reduced from those reported in the current recommendations for $O(^1D)$ kinetics for use in atmospheric modeling¹ (Table 2). Examples of the experimental results are presented below, whereas detailed summaries of the results for each of the 11 halocarbons included in this work are provided in the Supporting Information. The trend in $O(^1D)$ reactivity with halocarbon composition is also discussed briefly.

A representative set of OH temporal profiles measured in the determination of the total rate coefficient, $k_T(296 \text{ K})$, for the $O(^1D) + \text{CF}_3\text{CF}_2\text{Cl}$ (CFC-115) reaction is shown in Figure 1. The OH temporal profiles obtained under other experimental conditions and for the other halocarbons were of similar quality and precision to those shown in Figure 1 (see Supporting Information). The overall precision of the measurements was

high, and the OH radical temporal profiles show a systematic increase in the rate of rise and a general decrease in the total OH radical production with increasing halocarbon concentration. Nonlinear least-squares fits of the OH radical profiles to eq II are included in Figure 1, and in all cases the fits reproduced the experimental data to within the precision of the measurements. The obtained ($k_{\text{rise}} - k_0$) values from several independent experiments are shown in Figure 2 for the CF₃CF₂Cl (CFC-115) reaction. The agreement among the independent experiments was good and a least-squares fit of the combined data set yielded $k_T(296 \text{ K})$ for the $O(^1D) + \text{CF}_3\text{CF}_2\text{Cl}$ (CFC-115) reaction; see results given in Table 1.

$k_T(T)$ was measured over the temperature range 217–373 K for each of the 11 halocarbons. A summary of the experimental conditions and rate coefficient results is given in Table 1. The $O(^1D)$ atom reaction with CF₂Cl₂ (CFC-12), CF₂ClCF₂Cl (CFC-114), CF₃CF₂Cl (CFC-115), CHF₃ (HFC-23), CHF₂CF₃ (HFC-125), CH₃CF₃ (HFC-143a), and CF₃CHFCF₃ (HFC-227ea) showed weak, but measurable, temperature dependence in $k_T(T)$. For the other halocarbons, $k_T(T)$ showed no measurable dependence on temperature within the precision of the measurement. The measured $k_T(T)$ values were fit to an Arrhenius expression, $k_T(T) = A \exp(-E/RT)$, and the obtained pre-exponential A factors and E/R values are given in Table 2 along with the measured $k_T(296 \text{ K})$ values (Arrhenius plots for all the halocarbons are given in the Supporting Information).

Reactive rate coefficients, k_R for CFCl₃ (CFC-11), CF₃CClF₂ (CFC-115), CHF₂Cl (HCFC-22), CH₃CF₂Cl (HCFC-142b), CHF₃ (HFC-23), CHF₂CF₃ (HFC-125), CH₃CF₃ (HFC-143a), and CF₃CHFCF₃ (HFC-227ea) were measured at 296 K. A representative set of relative rate data for the $O(^1D) + \text{CF}_3\text{CF}_2\text{Cl}$ (CFC-115) reaction is shown in Figure 3, where experimental

Table 4. Summary of Reactive Yields for the O(¹D) + Halocarbon Reactions Obtained in This Work and the Results Available from Earlier Studies

halocarbon		reactive yield ^a	quenching yield	CIO yield	OH yield	exptl method ^b	ref
CFCl ₃	CFC-11	0.90 ± 0.07	0.12 ± 0.04	0.88 ± 0.18 0.79 ± 0.04		RR	this work
						RA	Force and Wiesenfeld ¹¹
						LIF	Takahashi et al. ¹²
						CRDS	Feierabend et al. ¹³
CF ₂ Cl ₂	CFC-12		0.14 ± 0.07 0.19 ± 0.05	0.87 ± 0.18 0.76 ± 0.06 0.80 ± 0.10		RA	Force and Wiesenfeld ¹¹
						LIF	Takahashi et al. ¹²
						CRDS	Feierabend et al. ¹³
						CRDS	Baasandorj et al. ⁸
CFCl ₂ CF ₂ Cl	CFC-113					CRDS	Baasandorj et al. ⁸
CF ₂ ClCF ₂ Cl	CFC-114		0.25 ± 0.09			RF	Ravishankara et al. ¹⁴
CF ₃ CF ₂ Cl	CFC-115		0.70 ± 0.07	0.85 ± 0.12		CRDS	Baasandorj et al. ⁸
						RF	Ravishankara et al. ¹⁴
						RR	this work
						RR	Atkinson et al. ²⁰
CHF ₂ Cl	HCFC-22	2 1		0.55 ± 0.1 0.28 ± 0.06 0.56 ± 0.03		RA/A	Addison et al. ^{16c}
						RF	Warren et al. ¹⁵
						CRDS	Feierabend et al. ¹³
						RR	this work
CH ₃ CF ₂ Cl	HCFC-142b	0.77 ± 0.06 0.76 ± 0.19 0.60 ± 0.04		0.26 ± 0.05		RR	Green and Wayne ¹⁷
						RF	Warren et al. ¹⁵
						RR	this work
						RR	Force and Wiesenfeld ¹¹
CHF ₃	HFC-23		0.77 ± 0.12 1.02 ± 0.03			RF	Schmoltner et al. ¹⁸
						RF	this work
						RR	Green and Wayne ¹⁷
						RR	Warren et al. ¹⁵
CHF ₂ CF ₃	HFC-125	1.5	0.85(+0.15/−0.22) 0.24 ± 0.04		0.6 ± 0.1	RF	Kono and Matsumi ¹⁹
						LIF	this work
						RR	Green and Wayne ¹⁷
						RR	Green and Wayne ¹⁷
CH ₃ CF ₃	HFC-143a	0.73 ± 0.09 1.1	0.18 ± 0.04		0.38 ± 0.06	LIF	Kono and Matsumi ¹⁹
						RR	this work
						RR	this work
						RR	this work
CF ₃ CHFCF ₃	HFC-227ea	0.72 ± 0.07				RR	this work

^aUncertainties reported for “this work” are 2σ from the measurement precision. ^bAll studies used pulsed laser photolysis to produce O(¹D) combined with the detection methods given in the table. Key: RR, relative rate technique; RF, atomic resonance fluorescence; RA, resonance absorption; CRDS, cavity ring-down spectroscopy; LIF, laser induced fluorescence; A, transient absorption. ^cAlso reported yields for CF₂ (0.45 ± 0.10), O(³P) (0.28 +0.10/−0.15), and OH (0.05) with O(³P) from the reaction channel yielding CF₂ and HCl.

results obtained using three different reference compounds are shown. The loss of the reactant halocarbon relative to that of the reference compound obeyed eq 1 in all cases. In general, there was very good agreement in the k_R values obtained in experiments performed using different reference compounds; the agreement was better than 10%. The results obtained in the relative rate experiments for all the halocarbons are summarized in Table 3. As a result of the high precision of the present relative rate measurements, the absolute uncertainty in $k_R(296\text{ K})$ is primarily determined by the absolute uncertainty in the N₂O and NF₃ reference reaction rate coefficients (Table 3), which are estimated to be ±20% at the 2σ level of uncertainty. The present results are scalable if the reference rate coefficients used in this work are revised in the future.

The reactive yields, $k_R(296\text{ K})/k_T(296\text{ K})$, obtained using the combined results from this work are compared with previously reported reaction product yields and quenching branching ratios in Table 4. It should be noted that reactive yields from this work are provided primarily for comparison purposes, whereas the measured k_R values, which are independent of k_T , should be used for input in atmospheric model calculations.

3.1. O(¹D) + Chlorofluorocarbons (CFCs). Total rate coefficients, $k_T(T)$, were measured in this work for the chlorofluorocarbons (CFCs): CFCl₃ (CFC-11), CF₂Cl₂ (CFC-12), CF₂ClCFCl₂ (CFC-113), CF₂ClCF₂Cl (CFC-114), and CF₃CF₂Cl (CFC-115). $k_T(296\text{ K})$ for the CFCl₃ (CFC-11) and CF₂Cl₂ (CFC-12) reactions agree well with values reported in the earlier studies of Davidson et al.¹⁰ and Force and Wiesenfeld,¹¹ where agreement is to within ~9%. $k_R(T)$ was measured for the CFCl₃ (CFC-11) reaction at 240 and 296 K with N₂O as the reference compound and found to be independent of temperature to within the precision of the measurement, ~5%. A reactive yield of (0.90 ± 0.07) was obtained for this reaction using the present results, which is consistent with the CIO yields of 0.88 ± 0.18 and 0.79 ± 0.04 reported by Takahashi et al.¹² and Feierabend et al.,¹³ respectively. The CIO radical product channel is expected to be the major, if not the only, reactive channel in this reaction; this implies 5–20% O(¹D) quenching in this reaction. Our measured k_R is also consistent with the O(¹D) quenching branching ratio reported by Force and Wiesenfeld¹¹ of 0.12 ± 0.04. Therefore, the available data for the CFC-11 and CFC-12 reactions are in good agreement where the estimated 2σ uncertainties in $k_T(T)$

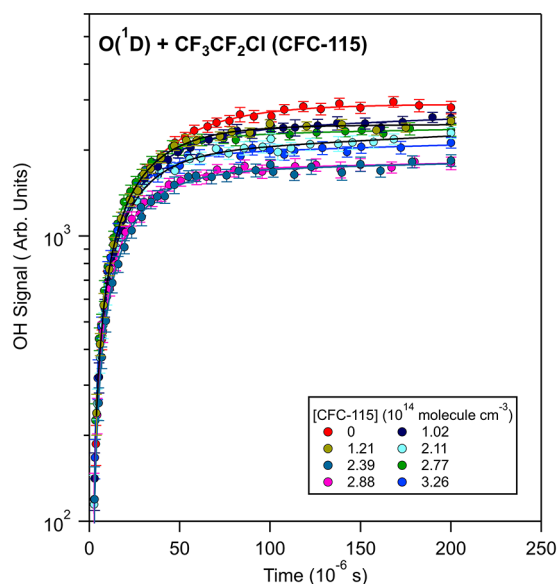


Figure 1. $O(^1D) + CF_3CF_2Cl$ (CFC-115) reaction kinetic data obtained using the competitive reaction method (see text for details). Representative OH radical temporal profiles are obtained at 296 K and 35 Torr (He) for a range of CF_3CF_2Cl (CFC-115) concentrations as given in the legend. The lines are nonlinear least-squares fits of the OH temporal profiles (see text).

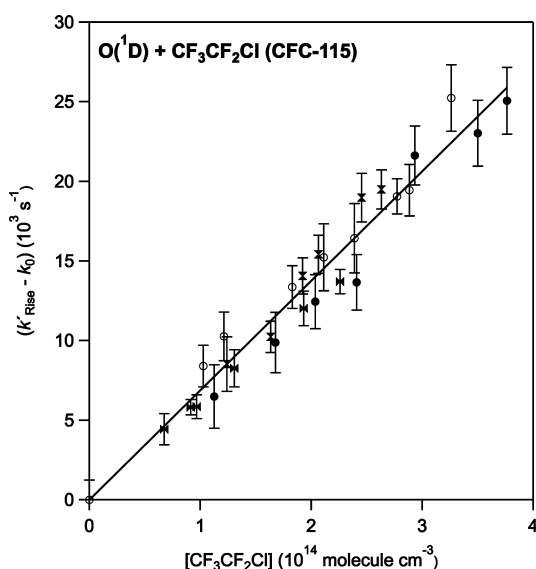


Figure 2. Pseudo-first-order rate coefficient data, $k'_{Rise} - k_0$, obtained for the $O(^1D) + CF_3CF_2Cl$ (CFC-115) reaction in three independent experiments. The line is a linear least-squares fit of the data. The experimental conditions and results are summarized in Table 1.

and $k_R(296\text{ K})$ from the precision of the present work are 8 and 5%, respectively. On the basis of the limited temperature dependence measurements performed in this work for the CFC-11 reaction and for CFC-12 in a previous study from this laboratory by Feierabend et al.,¹³ the change in the reactive yield over the temperature range 200–296 K is expected to be minor, <5%, for the halocarbons included in this study.

$k_T(296\text{ K})$ for the $CF_2ClCFCl_2$ (CFC-113) and CF_2ClCF_2Cl (CFC-114) reactions are in good agreement with our recently reported values.⁸ The present measurements, however, have extended the temperature range of the kinetic measurements

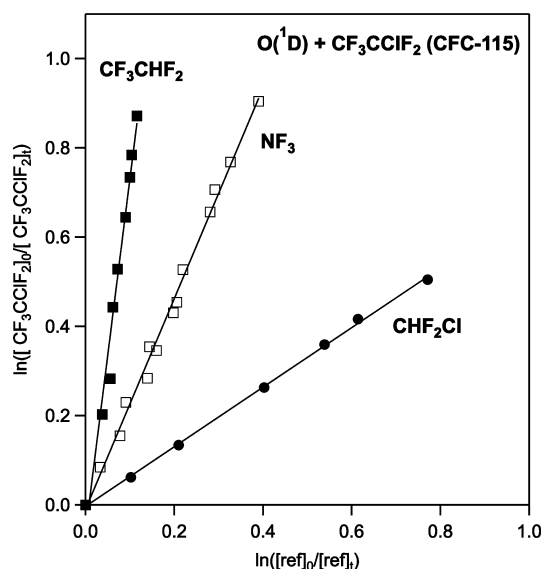


Figure 3. Reactive rate coefficient data for the $O(^1D) + CF_3CF_2Cl$ (CFC-115) reaction obtained at 296 K with CHF_2Cl (HCFC-22), NF_3 , and CF_3CHF_2 (HFC-125) as reference compounds (see text for details). The lines are linear least-squares fits to the data. The obtained rate coefficient ratios and k_R values are summarized in Table 3.

and found a weak negative temperature dependence, $E/R = -(25 \pm 50)$, for the CF_2ClCF_2Cl (CFC-114) reaction.

Our measured $k_T(296\text{ K})$ for the CF_3CF_2Cl (CFC-115) reaction is ~40% greater than the value reported by Ravishankara et al.¹⁴ This difference is greater than the combined 2σ uncertainties of the two measurements and the reason for this discrepancy is unknown. $k_R(296\text{ K})$ for this reaction was measured with NF_3 , CF_3CHF_2 (HFC-125), and CHF_2Cl (HCFC-22) used as reference compounds (Figure 3). The individual $k_R(296\text{ K})$ values are in very good agreement (Table 3), with an average reactive rate coefficient of $(5.16 \pm 0.18) \times 10^{-11}\text{ cm}^3\text{ molecule}^{-1}\text{ s}^{-1}$. Our $k_R(296\text{ K})$ value is actually slightly greater than the value of $k_T(296\text{ K})$ reported by Ravishankara et al.,¹⁴ $(5.0 \pm 0.4) \times 10^{-11}\text{ cm}^3\text{ molecule}^{-1}\text{ s}^{-1}$, which implies a possible error in their $k_T(296\text{ K})$ value, and a factor of 3 greater than the $k_R(296\text{ K})$ value derived from their reported $O(^1D)$ quenching yield. Taking $k_R(296\text{ K})$ and $k_T(296\text{ K})$ measured in this work gives a reactive yield of 0.73 ± 0.03 . This result contradicts the large $O(^1D)$ quenching yield, 0.70 ± 0.07 , reported for the $O(^1D) + CF_3CF_2Cl$ (CFC-115) reaction by Ravishankara et al.,¹⁴ which is currently recommended for use in atmospheric models.¹ Using the present results in model calculations significantly alters the calculated atmospheric lifetime for CFC-115 as described in the Atmospheric Implications section below.

3.2. $O(^1D) +$ Hydrochlorofluorocarbons (HCFCs). $k_T(T)$ and $k_R(296\text{ K})$ were measured for the hydrochlorofluorocarbons (HCFCs) CHF_2Cl (HCFC-22), and CH_3CF_2Cl (HCFC-142b). $k_T(296\text{ K})$ for the $O(^1D) + CHF_2Cl$ (HCFC-22) reaction is in good agreement, to within 8%, with the results from the studies of Davidson et al.¹⁰ and Warren et al.¹⁵ Davidson et al.¹⁰ also reported $k_T(T)$ over the temperature range 173–343 K. Their study extended to temperatures lower than included in the present work and established a rate coefficient temperature dependence, $E/R = -(50 \pm 50)\text{ K}$. The present measurements are of higher precision than the Davidson et al. study and a least-squares fit yields $E/R = 0 \pm 50\text{ K}$.

The present measurements, therefore, do not differ significantly from the current recommendations¹ (Table 2), but lead to a considerable reduction in the overall estimated uncertainties in $k_T(T)$ and k_R .

$k_R(296\text{ K})$ for the CHF_2Cl (HCFC-22) reaction was determined using NF_3 as the reference compound (Table 3). $k_R(296\text{ K})$ and $k_T(296\text{ K})$ from this work for the CHF_2Cl (HCFC-22) reaction yielded a reactive branching ratio of 0.77 ± 0.03 . This agrees with the $\text{O}(^1\text{D})$ quenching yield of 0.28 ± 0.06 reported by Warren et al.¹⁵ to within the combined 2σ uncertainties of the measurements. The reactive yield is greater than the ClO radical yield of 0.56 ± 0.03 and 0.55 ± 0.1 reported by Feierabend et al.¹³ and Addison et al.,¹⁶ respectively (Table 4). The difference implies that $\sim 20\%$ of the total reaction proceeds through a H-atom abstraction channel, although direct measurements of the OH radical yield are currently not available in the literature. We recommend a 0.56 reactive yield for the ClO radical and a 0.21 yield for the OH radical should be used in atmospheric model calculations.

$k_T(296\text{ K})$ for the $\text{O}(^1\text{D}) + \text{CH}_3\text{CF}_2\text{Cl}$ (HCFC-142b) reaction is $\sim 15\%$ less than reported by Warren et al.,¹⁵ which is the only other measurement of $k_T(296\text{ K})$. The combined 2σ uncertainty limits from the two studies overlap slightly. The present work established that this reaction has a negligible temperature dependence, $E/R = 0 \pm 45\text{ K}$, between 217 and 374 K. $k_R(296\text{ K})$ was measured using CHF_2Cl (HCFC-22) and $\text{CF}_3\text{CF}_2\text{Cl}$ (CFC-125) as reference compounds, which yielded $k_R(296\text{ K})$ values that agreed to within 8%. An average value is reported in Table 3. The relative rate study of Green and Wayne¹⁷ yields a higher reactive branching ratio, 0.76 ± 0.19 , when combined with $k_T(296\text{ K})$ from this work, although it agrees with the present results within the combined 2σ uncertainty limits. Warren et al.¹⁵ reported a $\text{O}(^1\text{D})$ quenching yield of 0.26 ± 0.05 , which corresponds to a reactive yield that falls slightly outside the combined uncertainty limits with the present work. The reason for this discrepancy is unknown. It is likely that both ClO and OH radicals are formed as products in this reaction, although no experimental measurements are currently available. As discussed below, it is expected that the ClO radical yield would be greater than the OH radical yield in this reaction.

3.3. $\text{O}(^1\text{D}) + \text{Hydrofluorocarbons (HFCs)}$. $k_T(T)$ and $k_R(296\text{ K})$ were measured for the hydrofluorocarbons (HFCs) CHF_3 (HFC-23), CHF_2CF_3 (HFC-125), CH_3CF_3 (HFC-143a), and $\text{CF}_3\text{CHF}_2\text{CF}_3$ (HFC-227ea) and the results are described separately below.

$k_T(296\text{ K})$ for the $\text{O}(^1\text{D}) + \text{CHF}_3$ (HFC-23) reaction is 10% greater than the value reported by Force and Wiesenfeld¹¹ and in good agreement with the value reported by Schmoltner et al.,¹⁸ to within 2% (Table 2). $k_T(T)$ was measured at five temperatures in the range 217–374 K and showed a weak negative temperature dependence, $E/R = -(30 \pm 10)$. The agreement with previous results combined with the high precision of the present work enable a significant reduction in the estimated uncertainties for this reaction (Table 2).

$k_R(296\text{ K})$ for CHF_3 (HFC-23) was measured using NF_3 as the reference compound. The average of three independent experimental measurements yielded a rate coefficient ratio of 0.105 ± 0.002 . Taking our $k_T(296\text{ K})$ value gives a reactive yield of 0.24 ± 0.04 , which is consistent with that inferred from the measured $\text{O}(^1\text{D})$ quenching yield of 0.77 ± 0.12 reported by Force and Wiesenfeld.¹¹ In a more recent study, Schmoltner et al.¹⁸ reported a $\text{O}(^1\text{D})$ quenching yield of 1.02 ± 0.03 , i.e.,

no measurable reactive channel. It is clear from our relative rate experiments that there is a significant reactive component to this reaction in contrast to the Schmoltner et al. study. In part, as a result of the discrepancy in the Force and Wiesenfeld and Schmoltner et al. results there was not a recommendation given in the NASA/JPL evaluation for use in atmospheric modeling.¹ Including a $\text{O}(^1\text{D})$ reactive loss for CHF_3 (HFC-23) in atmospheric models primarily impacts its local stratospheric lifetime as discussed in the Atmospheric Implications section below.

$k_T(296\text{ K})$ for the $\text{O}(^1\text{D}) + \text{CHF}_2\text{CF}_3$ (HFC-125) reaction was measured in this work to be $(0.101 \pm 0.004) \times 10^{-10}\text{ cm}^3\text{ molecule}^{-1}\text{ s}^{-1}$. Previously reported values of $k_T(296\text{ K})$ from studies by Warren et al.¹⁵ and Kono and Matsumi¹⁹ differ greatly, by nearly a factor of 10 (Table 2). Our $k_T(296\text{ K})$ value is in good agreement with the value of $0.100 (+0.01/-0.005) \times 10^{-10}\text{ cm}^3\text{ molecule}^{-1}\text{ s}^{-1}$ reported by Kono and Matsumi.¹⁹ $k_T(T)$ was measured in our work at four temperatures between 217 and 373 K and found to have a weak negative temperature dependence, $E/R = -(25 \pm 30)$. The present work resolves the large discrepancy in the previously reported values of $k_T(296\text{ K})$ and the high precision of the present results enables a significant reduction in the estimated uncertainties.

$k_R(296\text{ K})$ for the CHF_2CF_3 (HFC-125) reaction was measured using CHF_3 and NF_3 as reference compounds. The results from the two reference compounds agreed to within 15% (Table 3), and the average value corresponds to a reactive yield of 0.73 ± 0.09 when combined with our $k_T(296\text{ K})$. There are three previous studies, which are listed in Table 4, with which to compare our results. The relative rate study of Green and Wayne¹⁷ would correspond to a reactive yield substantially greater than 1 and, therefore, seems to be in error. Warren et al.¹⁵ report a high $\text{O}(^1\text{D})$ quenching yield for this reaction, $0.85 (+0.15/-0.22)$, whereas Kono and Matsumi¹⁹ report a much lower value, 0.24 ± 0.04 , and a high OH radical yield, 0.6 ± 0.1 . The present results are in good agreement with the results from the Kono and Matsumi study for the overall reactive yield. The reason for the large discrepancy with the Warren et al. study is unknown. The NASA/JPL recommendation¹ for the CHF_2CF_3 (HFC-125) reaction was based on the values reported by Warren et al.,¹⁵ which has been shown in the present study to be in error. It should be noted, however, that the errors in the $k_T(298\text{ K})$ and $k_R(296\text{ K})$ values reported in the Warren et al. study offset in atmospheric model calculated lifetimes. Therefore, although the rate coefficient recommendations require major revision the overall impact on calculated atmospheric lifetimes may not be as large, as shown in the Atmospheric Implications section below.

$k_T(298\text{ K})$ for the CH_3CF_3 (HFC-143a) reaction was measured to be $\sim 45\%$ greater than the value reported by Kono and Matsumi¹⁹ (Table 2). The level of agreement between the results from the present work and that of Kono and Matsumi for the other halocarbons common to the two studies is in most cases better than this. The reason for the discrepancy for CH_3CF_3 (HFC-143a) is unknown. $k_T(T)$ was measured in this work at five temperatures between 217 and 373 K and the high precision of the measurements yielded a weak negative temperature dependence in $k_T(T)$, $E/R = -(20 \pm 25)$.

Due in part to the discrepancies in the measurements of $k_T(T)$ for the CH_3CF_3 (HFC-143a) reaction, $k_R(296\text{ K})$ was measured in the present work using NF_3 , $\text{CF}_3\text{CF}_2\text{Cl}$ (CFC-115), and CHF_2Cl (HCFC-22) as reference compounds. The results obtained using the different reference compounds were in good

agreement (Table 3), where the spread in the obtained $k_R(296\text{ K})$ values was $\sim 13\%$ and the average value was $(0.391 \pm 0.011) \times 10^{-10} \text{ cm}^3 \text{ molecule}^{-1} \text{ s}^{-1}$; this corresponds to a reactive yield of 0.55 ± 0.04 . The study of Green and Wayne¹⁷ reported a reactive yield of 1.1 for this reaction. The study of Kono and Matsumi¹⁹ reported a $\text{O}(^1\text{D})$ quenching yield of 0.18 ± 0.04 and a OH radical yield of 0.38 ± 0.06 . Therefore, the available experimental results of the reactive yield for this reaction are in poor agreement. The good agreement in the $k_R(296\text{ K})$ values obtained in this work for three different reference compounds gives us confidence in the value measured in this work, although the product yields for this reaction are more uncertain.

To the best of our knowledge $k_T(T)$ and $k_R(296\text{ K})$ for the $\text{O}(^1\text{D}) + \text{CF}_3\text{CHF}_2\text{CF}_3$ (HFC-227ea) reaction have not been reported previous to this study. The reactive yield in this reaction is high, 0.72 ± 0.07 , and is similar to that for the $\text{O}(^1\text{D}) + \text{CHF}_2\text{CF}_3$ (HFC-125) reaction measured in this work. The $\text{O}(^1\text{D})$ reaction represents a stratospheric loss process for this molecule as discussed below.

3.4. Trends in $\text{O}(^1\text{D})$ Reactivity. An examination of the $\text{O}(^1\text{D}) + \text{halocarbon}$ rate coefficients obtained in the present study, Tables 1–4, as well as those from previous studies,¹ show a systematic trend in $k_R(296\text{ K})$ in which reactivity increases with increasing H- and Cl-atom substitution. Previous studies have shown that perfluorinated compounds are unreactive, $k_R(296\text{ K})$ values $< 1 \times 10^{-14} \text{ cm}^3 \text{ molecule}^{-1} \text{ s}^{-1}$,^{5,14} as the abstraction of a F-atom is endothermic. The extent of fluorination influences $k_R(296\text{ K})$ for a halocarbon not only through occupying reactive sites but also via the inductive effect of a F-atom or CF_3 group on the C–H or C–Cl bonds. The greatest inductive effect is for substitution on the α -carbon; fluorination at a β site is substantially less influential. For example, the results from our study show that CHF_2CF_3 (HFC-125) and $\text{CF}_3\text{CHF}_2\text{CF}_3$ (HFC-227ea), which each contain a single H-atom available for abstraction, have similar $k_T(296\text{ K})$ and $k_R(296\text{ K})$ values, 0.0733×10^{-10} and $0.0699 \times 10^{-10} \text{ cm}^3 \text{ molecule}^{-1} \text{ s}^{-1}$, respectively. $k_R(296\text{ K})$ for CHF_3 (HFC-23), however, is approximately a factor of 3 less, $0.022 \times 10^{-10} \text{ cm}^3 \text{ molecule}^{-1} \text{ s}^{-1}$, although its $k_T(296\text{ K})$ value is similar to those for CHF_2CF_3 (HFC-125) and $\text{CF}_3\text{CHF}_2\text{CF}_3$ (HFC-227ea). This difference most likely reflects the increased fluorine inductive effect; the C–H bond strength in CHF_3 (HFC-23) is $\sim 3 \text{ kcal mol}^{-1}$ stronger than in CHF_2CF_3 (HFC-125). $k_R(296\text{ K})$ for the CH_3CF_3 (HFC-143a) reaction is consistent with this trend, although $k_R(296\text{ K})$ is greater, $0.391 \times 10^{-10} \text{ cm}^3 \text{ molecule}^{-1} \text{ s}^{-1}$, primarily due to the greater number of available H-atoms for abstraction. Although it is difficult to assign a specific rate coefficient, each H-atom in a halocarbon molecule contributes $(0.05\text{--}0.13) \times 10^{-10} \text{ cm}^3 \text{ molecule}^{-1} \text{ s}^{-1}$ to the overall $k_R(296\text{ K})$ value.

The effective $k_R(296\text{ K})$ for a Cl-atom abstraction is significantly greater than that for a H-atom. It is also less sensitive to the degree of fluorination, e.g., $k_R(296\text{ K})$ for CFCl_3 (CFC-11) and $\text{CF}_3\text{CF}_2\text{Cl}$ (CFC-115) roughly scale with the number of available Cl atoms, although the degree of fluorination is significantly different. $k_R(296\text{ K})$ values per Cl atom fall in the range $(0.5\text{--}0.7) \times 10^{-10} \text{ cm}^3 \text{ molecule}^{-1} \text{ s}^{-1}$ for the halocarbons studied here.

The high precision of the present measurements enabled the determination that a majority of the $\text{O}(^1\text{D})$ reactions in this study displayed a weak negative temperature dependence in $k_T(T)$. Reactions having a weak negative temperature dependence

implies the formation of a prereactive complex in the reaction mechanism. The formation of reactive complexes has been proposed previously (see Kono and Matsumi¹⁹ and references within), but experimental evidence supporting this hypothesis is rather limited.

4. ATMOSPHERIC IMPLICATIONS

Reaction with the $\text{O}(^1\text{D})$ atom is primarily a stratospheric loss process. Other atmospheric loss processes, such as reaction with the OH radical and UV photolysis, are also important tropospheric and stratospheric loss processes for the halocarbons considered in this work; UV photolysis in the stratosphere is a dominant loss process for the chlorine containing CFCs and HCFCs, whereas the OH reaction is important throughout the troposphere and stratosphere for the hydrogen containing HCFCs and HFCs. The $\text{O}(^1\text{D})$ reaction, therefore, is expected to be a secondary loss process for the majority of the molecules included in this study, particularly for molecules with atmospheric lifetimes less than ~ 50 years. In this work, the Goddard Space Flight Center (GSFC) 2D atmospheric model^{2,3} was used to evaluate the local and global annually averaged lifetimes of the compounds included in this study and the fractional contribution of the $\text{O}(^1\text{D})$ reaction to their atmospheric loss. The range in the calculated lifetime due solely to the uncertainty in the $\text{O}(^1\text{D})$ kinetics was also quantified using the 2D model calculations. The model calculated lifetimes are compared with values calculated using the $\text{O}(^1\text{D})$ kinetic parameters currently recommended for use in atmospheric modeling by the NASA/JPL data evaluation panel.¹

Model runs were performed using the $\text{O}(^1\text{D})$ kinetics from the present work while holding other model input to the NASA/JPL recommended values. Base model runs were also performed using the NASA/JPL recommended input kinetic and photochemical parameters. The range in atmospheric lifetimes was calculated using the high and low rate coefficient values determined from the 2σ estimated uncertainty limits in k_R from this work; k_R is the most relevant $\text{O}(^1\text{D})$ kinetic parameter for the calculation of a molecules atmospheric loss rate.

The greatest differences in $k_R(296\text{ K})$ between the present work and the NASA/JPL recommendations are found for the $\text{CF}_3\text{CF}_2\text{Cl}$ (CFC-115) and CHF_3 (HFC-23) reactions, where the differences are factors of ~ 3.5 and ~ 7 , respectively. The differences for the $\text{CF}_2\text{ClCFCl}_2$ (CFC-113), $\text{CF}_2\text{ClCF}_2\text{Cl}$ (CFC-114), CH_3CClF_2 (HCFC-142b), and CHF_2CF_3 (HFC-125) reactions are less, but still significant, with differences in the 12–23% range. There is currently very limited experimental data for the temperature dependence of the reactive rate coefficient, $k_R(T)$. Results from this work for the CFCl_3 (CFC-11) reaction and previous work from our laboratory¹³ for the CF_2Cl_2 (CFC-12) reaction observed no significant temperature dependence in k_R and the reactive yield, respectively. It was, therefore, assumed in the 2D model calculations that k_R was temperature independent.

The estimated uncertainties in $k_R(296\text{ K})$ from the present work are 10%, or less, and are significantly less than the NASA/JPL recommended values (see Table 2 for a comparison of the estimated uncertainty factors). The difference in estimated uncertainties are substantially greater at reduced temperatures where the uncertainties obtained in the present work are nearly a factor of 10 less for the majority of the reactions studied. The reduction of uncertainty leads to significantly reduced

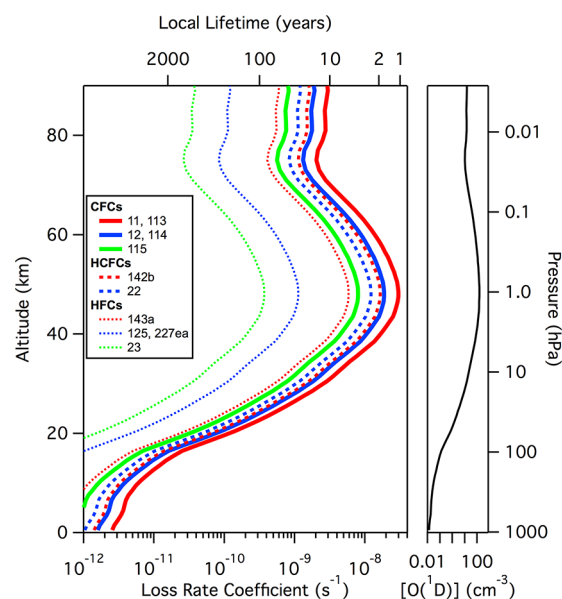


Figure 4. Vertical profiles of the atmospheric first-order loss rate coefficients, $k_R[\text{O}(^1\text{D})]$, for the $\text{O}(^1\text{D})$ + halocarbon reactions included in this work (see legend) calculated using the GSFC 2D model and the reactive rate coefficients, k_R , from this work. The right-hand panel shows the model calculated global annually averaged $\text{O}(^1\text{D})$ vertical profile.

uncertainty in the model calculated stratospheric local loss rates for the $\text{O}(^1\text{D})$ reaction.

The global annually averaged $\text{O}(^1\text{D})$ vertical concentration profile calculated from the 2D model is shown in Figure 4; the concentration reaches a maximum of $\sim 100 \text{ atom cm}^{-3}$ near 45 km. The calculated first-order loss rates, $k_R[\text{O}(^1\text{D})]$, for the halocarbons included in this work are also shown in Figure 4. The mesospheric (~ 50 – 90 km region) loss due to $\text{O}(^1\text{D})$ reaction is significant; however, the atmospheric abundances of the CFCs, HCFCs, and HFCs are very small in this region of the atmosphere. Thus, the contribution of the mesospheric loss to the atmospheric lifetime is minor for most of the halocarbons considered here. The exception is $\text{CF}_3\text{CF}_2\text{Cl}$ (CFC-115) for which the mesospheric loss contributes about 10% to its overall loss. The shape of the vertical profiles for the different molecules are very similar due to the weak temperature dependence for the $\text{O}(^1\text{D})$ reactions, and the difference in k_R values for the CFCs, HCFCs, and HFCs is reflected as the difference in the magnitude of the altitude dependent loss rates. The local lifetimes are a minimum near the $[\text{O}(^1\text{D})]$ maximum at ~ 45 km with the shortest local lifetimes being in the range of 1 to 2 years, e.g., for several of the CFCs and $\text{CH}_3\text{CF}_2\text{Cl}$ (HCFC-142b). The compounds with the longest local lifetime are the highly fluorinated HFCs CHF_3 (HFC-23), CHF_2CF_3 (HFC-125), and $\text{CF}_3\text{CHF}_2\text{CF}_3$ (HFC-227ea).

Table 5. Atmospheric Fractional Losses and Lifetimes Calculated for Year 2000 Steady-State Conditions Using the GSFC 2D Model for the Molecules Included in This Study

halocarbon		fractional loss			lifetime (years)			
					this work			NASA/JPL
					tropospheric ^b	stratospheric ^b	mesospheric ^b	global ^b
		$\text{O}(^1\text{D})^a$	OH	$h\nu$				global ^c
CFCl_3	CFC-11	0.018 (0.019)	0.002	0.980	1524 (1480–1565)	62.9 (62.8–62.9)	>50000	60.4 (60.3–60.5)
CF_2Cl_2	CFC-12	0.053 (0.051)	0.006	0.941	5910 (5689–6127)	108.7 (108.5–108.8)	>50000	106.7 (106.4–106.8)
$\text{CFCl}_2\text{CF}_2\text{Cl}$	CFC-113	0.062 (0.067)		0.938	5994 (5534–6466)	100.1 (99.88–100.3)	>50000	98.5 (98.1–98.8)
$\text{CF}_2\text{ClCF}_2\text{Cl}$	CFC-114	0.219 (0.249)		0.781	21160 (18450–24220)	233.9 (229.4–237.8)	2882.0 (2819–2954)	214.1 (210–217)
$\text{CF}_3\text{CF}_2\text{Cl}$	CFC-115	0.673 (0.365)		0.327	36440 (31180–42870)	664.1 (607.4–726.9)	4810 (4642–4989)	574 (528–625)
CHClF_2	HCFC-22	0.011 (0.013)	0.987	0.002	12.7 (12.7–12.7)	240.0 (235.5–244.2)	4993 (4939–5048)	12.1 (12.0–12.1)
CH_3CClF_2	HCFC-142b	0.027 (0.041)	0.959	0.014	19.1 (19.0–19.1)	256.50 (249.0–264.0)	3818.0 (3803.0–3837.0)	17.7 (17.6–17.7)
CHF_3	HFC-23	0.002 (0.085)	0.998		238.9 (238.9–238.9)	5286 (5249–5319)	73060 (72200–73830)	227.9 (227.8–227.9)
CHF_2CF_3	HFC-125	0.039 (0.050)	0.961		32.3 (32.21–32.30)	394.2 (363.90–425.9)	6045.0 (5603.0–6569)	29.7 (29.4–29.9)
CH_3CF_3	HFC-143a	0.024 (0.041)	0.976		54.5 (50.78–54.5)	835.0 (800.3–869.5)	11000 (10410–11610)	51.0 (50.8–51.1)
$\text{CF}_3\text{CHF}_2\text{CF}_3$	HFC-227ea	0.008	0.992		44.5 (44.5–44.5)	797.0 (779.1–813.3)	12820 (12350–13260)	42.0 (41.9–42.1)

^aFractional loss obtained using $\text{O}(^1\text{D})$ rate coefficients from this work with values in parentheses obtained using NASA/JPL evaluation¹ recommended $\text{O}(^1\text{D})$ rate coefficients. ^bGlobal annually averaged lifetimes obtained using $\text{O}(^1\text{D})$ rate coefficients taken from this work and other model input parameters taken from the NASA/JPL evaluation,¹ the values in parentheses are the range in lifetime calculated using the 2σ uncertainty extremes in the k_R . ^cGlobal annually averaged lifetimes obtained using $\text{O}(^1\text{D})$ rate coefficients from the NASA/JPL evaluation.¹ The values in parentheses are the range in lifetime calculated using the 2σ uncertainty extremes in the k_R from the NASA/JPL evaluation.

As mentioned earlier, the $O(^1D)$ reaction is a secondary loss process for many of the compounds considered here. Table 5 provides a breakdown of the model calculated fractional losses due to the $O(^1D)$ and OH reactions and UV photolysis for each of the compounds. The $O(^1D)$ reaction contributes only a few percent to the global annually averaged total loss for most of the compounds, but ~22 and ~67% for the atmospherically long-lived compounds CF_2ClCF_2Cl (CFC-114) and CF_2ClCF_3 (CFC-115), respectively. The fractional $O(^1D)$ loss for the NASA/JPL recommended kinetic parameters is included in Table 5 for comparison with the present work. In most cases the differences in the fractional loss between the present work and NASA/JPL are small due to the small differences in the $O(^1D)$ rate coefficient data. The largest differences are for the CF_3CF_2Cl (CFC-115) and CHF_3 (HFC-23) reactions due to the significant differences in k_R obtained in the present work as discussed in the Results and Discussion section. The global annually averaged tropospheric, stratospheric, mesospheric, and overall atmospheric lifetimes are given in Table 5. The overall lifetimes obtained using the present results are in most cases similar to the values obtained using the NASA/JPL recommendations (Table 5), with a few exceptions; the exceptions are for the long-lived CF_2ClCF_2Cl (CFC-114) and CF_3CF_2Cl (CFC-115) compounds that are lost primarily via $O(^1D)$ reaction.

The ranges in lifetime due to the uncertainty in the $O(^1D)$ kinetics are also given in Table 5. In most cases, the range in lifetime is relatively small. This is primarily due to the small contribution of the $O(^1D)$ reaction to the total atmospheric loss as shown by the fractional loss contributions given in Table 5 and the reduced level of uncertainty in the $O(^1D)$ kinetic data obtained in the present work. Using the present kinetic results, the uncertainties in the $O(^1D)$ reaction are expected to have a minor impact on calculated atmospheric lifetimes for the ODSs and GHGs included in this work.

5. CONCLUSIONS

The present kinetic study has refined the total and reactive rate coefficients for the $O(^1D)$ reaction with the following key atmospheric halocarbons: chlorofluorocarbons (CFCs) $CFCl_3$ (CFC-11), CF_2Cl_2 (CFC-12), $CFCl_2CF_2Cl$ (CFC-113), CF_2ClCF_2Cl (CFC-114), CF_3CF_2Cl (CFC-115); hydrochlorofluorocarbons (HCFCs) CHF_2Cl (HCFC-22), CH_3CClF_2 (HCFC-142b); and hydrofluorocarbons (HFCs) CHF_3 (HFC-23), CHF_2CF_3 (HFC-125), CH_3CF_3 (HFC-143a), and CF_3CHFCF_3 (HFC-227ea). This work reports temperature dependent kinetic data, over the temperature range 217–373 K, which was previously unavailable for many of these halocarbons. The total rate coefficient, i.e., the $O(^1D)$ atom loss, showed a weak temperature dependence for most of the halocarbon reactions (Table 2), and the present results enable a significant reduction in the estimated uncertainties in the rate coefficient data used in atmospheric models. The reactive rate coefficients obtained in this work, as summarized in Tables 3 and 4, show a general trend in reactivity where a hydrogen and chlorine atom contribute approximately 0.1 and $0.6 \times 10^{-10} \text{ cm}^3 \text{ molecule}^{-1} \text{ s}^{-1}$, respectively, to the halocarbons reactive rate coefficient.

The rate coefficient data reported here resolve significant discrepancies in previously reported values for the CF_2ClCF_2Cl (CFC-114), CF_3CF_2Cl (CFC-115), CHF_3 (HFC-23), and CHF_2CF_3 (HFC-125) reactions, provides new data for the CF_3CHFCF_3 (HFC-227ea) reaction, and also provides the

kinetic data needed to improve the accuracy of modeled stratospheric chemistry. As part of this work, 2D model calculations were used to evaluate the local and global annually averaged atmospheric lifetimes for each of the halocarbons included in this study (Table 5). In addition, the fractional contribution of the $O(^1D)$ reaction to the atmospheric loss of the halocarbon was determined (Table 5); the $O(^1D)$ reaction is a major loss process for CF_2ClCF_2Cl (CFC-114) and CF_3CF_2Cl (CFC-115) and a minor global loss process for the other halocarbons included in this study. The $O(^1D)$ kinetic data obtained in this study are recommended for use in future lifetime evaluations, in ozone depletion and global warming potential calculations, and as input to model calculations of ozone recovery and climate change.

■ ASSOCIATED CONTENT

Supporting Information

Graphical summaries of the total and reactive rate coefficients measured in this work including estimated uncertainties, comparison with results from previous studies and current recommendations for atmospheric modeling, and a summary of recommended rate coefficients. This material is available free of charge via the Internet at <http://pubs.acs.org>.

■ AUTHOR INFORMATION

Corresponding Author

*E-mail: James.B.Burkholder@noaa.gov.

Present Address

#Department of Soil, Water, and Climate, University of Minnesota, St. Paul, MN, 55108-6028.

Notes

The authors declare no competing financial interest.

■ ACKNOWLEDGMENTS

This work was supported in part by NOAA's Climate Goal and NASA's Atmospheric Composition: Laboratory Studies and Modeling and Analysis Programs.

■ REFERENCES

- (1) Sander, S. P.; Abbatt, J.; Barker, J. R.; Burkholder, J. B.; Friedl, R. R.; Golden, D. M.; Huie, R. E.; Kolb, C. E.; Kurylo, M. J.; Moortgat, G. K.; Orkin, V. L.; Wine, P. H. *Chemical Kinetics and Photochemical Data for Use in Atmospheric Studies*; Evaluation Number 17, JPL Publication 10-6; Jet Propulsion Laboratory, California Institute of Technology: Pasadena, CA, 2011; <http://jpldataeval.jpl.nasa.gov>.
- (2) Fleming, E. L.; Jackman, C. H.; Weisenstein, D. K.; Ko, M. K. W. The Impact of Interannual Variability on Multidecadal Total Ozone Simulations. *J. Geophys. Res.* **2007**, *112*, D10310 DOI: 10.1029/12006JD007953.
- (3) Fleming, E. L.; Jackman, C. H.; Stolarski, R. S.; Douglas, A. R. A Model Study of the Impact of Source Gas Changes on the Stratosphere for 1850–2100. *Atmos. Chem. Phys.* **2011**, *11*, 8515–8541.
- (4) Papadimitriou, V. C.; Portmann, R. W.; Fahey, D. W.; Mühle, J.; Weiss, R. F.; Burkholder, J. B. Experimental and Theoretical Study of the Atmospheric Chemistry and Global Warming Potential of SO_2F_2 . *J. Phys. Chem. A* **2008**, *112*, 12657–12666.
- (5) Baasandorj, M.; Hall, B. D.; Burkholder, J. B. Rate Coefficients for the Reaction of $O(^1D)$ with the Atmospherically Long-Lived Greenhouse Gases NF_3 , SF_5CF_3 , CHF_3 , C_2F_6 , $c-C_4F_8$, $n-C_5F_{12}$, and $n-C_6F_{14}$. *Atmos. Chem. Phys.* **2012**, *12*, 11753–11764.
- (6) Baasandorj, M.; Knight, G.; Papadimitriou, V. C.; Talukdar, R. K.; Ravishankara, A. R.; Burkholder, J. B. Rate Coefficients for the Gas-

Phase Reaction of the Hydroxyl Radical with $\text{CH}_2=\text{CHF}$ and $\text{CH}_2=\text{CF}_2$. *J. Phys. Chem. A* **2010**, *114*, 4619–4633.

(7) Papadimitriou, V. C.; Talukdar, R. K.; Portmann, R. W.; Ravishankara, A. R.; Burkholder, J. B. $\text{CF}_3\text{CF}=\text{CH}_2$ and (Z)- $\text{CF}_3\text{CF}=\text{CHF}$: Temperature Dependent OH Rate Coefficients and Global Warming Potentials. *Phys. Chem. Chem. Phys.* **2008**, *10*, 808–820.

(8) Baasandorj, M.; Feierabend, K. J.; Burkholder, J. B. Rate Coefficients and ClO Radical Yields in the Reaction of $\text{O}(^1\text{D})$ with $\text{CClF}_2\text{CCl}_2\text{F}$, CCl_3CF_3 , $\text{CClF}_2\text{CClF}_2$, and CCl_2FCF_3 . *Int. J. Chem. Kinet.* **2011**, *43*, 1–9.

(9) Atkinson, R.; Baulch, D. L.; Cox, R. A.; Crowley, J. N.; Hampson, R. F.; Hynes, R. G.; Jenkin, M. E.; Rossi, M. J.; Troe, J.; Wallington, T. J. Evaluated Kinetic and Photochemical Data for Atmospheric Chemistry: Volume IV - Gas Phase Reactions of Organic Halogen Species. *Atmos. Chem. Phys.* **2008**, *8*, 4141–4496.

(10) Davidson, J. A.; Schiff, H. I.; Brown, T. J.; Howard, C. J. Temperature Dependence of the Rate Constants for Reactions of $\text{O}(^1\text{D})$ Atoms with a Number of Halocarbons. *J. Chem. Phys.* **1978**, *69*, 4277–4279.

(11) Force, A. P.; Wiesenfeld, J. R. Collisional Deactivation of $\text{O}(^1\text{D}_2)$ by the Halomethanes. Direct Determination of Reaction Efficiency. *J. Phys. Chem.* **1981**, *85*, 782–785.

(12) Takahashi, K.; Wada, R.; Matsumi, Y.; Kawasaki, M. Product Branching Ratios for $\text{O}(^3\text{P})$ Atom and ClO Radical Formation in the Reactions of $\text{O}(^1\text{D})$ with Chlorinated Compounds. *J. Phys. Chem.* **1996**, *100*, 10145–10149.

(13) Feierabend, K. J.; Papanastasiou, D. K.; Burkholder, J. B. ClO Radical Yields in the Reaction of $\text{O}(^1\text{D})$ with Cl_2 , HCl, Chloromethanes, and Chlorofluoromethanes. *J. Phys. Chem. A* **2010**, *114*, 12052–12061.

(14) Ravishankara, A. R.; Solomon, S.; Turnipseed, A. A.; Warren, R. F. Atmospheric Lifetimes of Long-Lived Halogenated Species. *Science* **1993**, *259*, 194–199.

(15) Warren, R.; Gierczak, T.; Ravishankara, A. R. A Study of $\text{O}(^1\text{D})$ Reactions with CFC Substitutes. *Chem. Phys. Lett.* **1991**, *183*, 403–409.

(16) Addison, M. C.; Donovan, R. J.; Garraway, J. Reactions of $\text{O}(^2\text{D}_2)$ and $\text{O}(^2^3\text{P}_1)$ with Halogenomethanes. *Discuss. Chem. Soc., Faraday* **1979**, *67*, 286–296.

(17) Green, R. G.; Wayne, R. P. Relative Rate Constants for the Reactions of $\text{O}(^1\text{D})$ Atoms with Fluorochlorocarbons and with N_2O . *J. Photochem.* **1976/77**, *6*, 371–374.

(18) Schmoltner, A. M.; Talukdar, R. K.; Warren, R. F.; Mellouki, A.; Goldfarb, L.; Gierczak, T.; McKeen, S. A.; Ravishankara, A. R. Rate Coefficients for Reactions of Several Hydrofluorocarbons with OH and $\text{O}(^1\text{D})$ and their Atmospheric Lifetimes. *J. Phys. Chem.* **1993**, *97*, 8976–8982.

(19) Kono, M.; Matsumi, Y. Reaction Processes of $\text{O}(^1\text{D})$ with Fluoroethane Compounds. *J. Phys. Chem.* **2001**, *105*, 65–69.

(20) Atkinson, R.; Breuer, G. M.; Pitts, J. N., Jr. Tropospheric and Stratospheric Sinks for Halocarbons: Photooxidation, $\text{O}(^1\text{D})$ Atom, and OH Radical Reactions. *J. Geophys. Res.* **1976**, *81*, 5765–5770.